Surprisingly weak coordination between leaf structure and function among closely-related tomato species

Christopher D. Muir[1,2], Miquel À. Conesa[3], Emilio J. Roldán[3], Arántzazu Molins[3], Jeroni Galmés[3]

[1] Department of Biology, Indiana University, Bloomington, IN 47405, USA

[2] Biodiversity Research Centre and Botany Department, University of British Columbia, Vancouver, British Columbia V6T 1Z4, Canada

[3] Research Group on Plant Biology under Mediterranean Conditions, Departament de Biologia, Universitat de les Illes Balears, Ctra. Valldemossa km 7.5, E-07122, Palma de Mallorca, Spain.

Abstract

Natural selection may often favor coordination between different traits, or phenotypic integration, in order to most efficiently acquire and deploy scarce resources. As leaves are the primary photosynthetic organ in plants, many have proposed that leaf physiology, biochemistry, and anatomical structure are coordinated along a functional trait spectrum from fast, resource-acquisitive syndromes to slow, resource-conservative syndromes. However, the coordination hypothesis has rarely been tested at a phylogenetic scale most relevant for understanding rapid adaptation in the recent past or predicting evolutionary trajectories in response to climate change. To that end, we used a common garden to examine genetically-based coordination between leaf traits across 19 wild and cultivated tomato taxa. We found surprisingly weak integration between photosynthetic rate, leaf structure, biochemical capacity, and CO_2 diffusion, even though all were arrayed in the predicted direction along a 'fast-slow' spectrum. This suggests considerable scope for unique trait combinations to evolve in response to new environments or in crop breeding. In particular, we find that partially independent variation in stomatal and mesophyll conductance may allow a plant to improve water-use efficiency without necessarily sacrificing maximum photosynthetic rates. Our study does not imply that functional trait spectra or tradeoffs are unimportant, but that the many important axes of variation within a taxonomic group may be unique and not generalizable to other taxa.

Introduction

The ecology of organisms critically depends on their ability to obtain energy for growth and reproduction. In C_3 plants, both passive diffusion of CO_2 from the atmosphere to chloroplasts, via stomata and the leaf mesophyll, and biochemical capacity limit photosynthetic rates (Farquhar & Sharkey 1982; Parkhurst 1994; Evans *et al*. 2009; Flexas *et al*. 2015). Optimization theory predicts that these functions should be tightly coordinated: leaf anatomies that allow rapid diffusion of CO_2 should also have the biochemical capacity to take advantage of it and *vice versa* (Givnish 1986; Wright *et al*. 2004; Reich 2014). Natural selection on trait coordination, also known as phenotypic integration (Pigliucci 2003), should thus generate major functional trait spectra associated with different ecological strategies (Grime 1977; Westoby *et al*. 2002; Chave *et al*. 2009; Reich 2014). Indeed, intrinsic photosynthetic capacity varies widely between species, indicating that leaf-level CO_2 diffusion and biochemistry are major levers through which natural selection and crop breeders can alter plant performance and fitness in different environments. For example, selection might favor leaf traits that inhibit rapid CO_2 diffusion (e.g. lower stomatal density or thicker leaves) if doing so has an adaptive benefit, bringing about a tradeoff (e.g. sclerophyll leaves of species from water-limited environments [Medrano *et al*. 2009]). It is not clear whether most functional trait variation between species lies along a single major axis (e.g. fast-slow continuum [Reich 2014]) or orthogonally along multiple independent trait axes.

In particular, the presence of functional trait spectra has rarely been examined among closely-related species in a phylogenetic context (Edwards *et al*. 2014; Mason & Donovan 2015). However, for certain ecological questions, data on genetically-based variation among closely-related species, rather than broad comparisons across disparate families and plant functional types, are most appropriate (Donovan *et al*. 2014). Specifically, ecological diversification is not

always predictable because different groups of organisms find unique adaptive solutions, leading to multiple trait spectra. For example, the leaf economics spectrum (Wright *et al*. 2004) is not a one-size-fits-all trait axis, but rather a set of axes that vary between communities (Funk & Cornwell 2013) and taxa (Edwards et al. 2014; Mason & Donovan 2015). Second, the evolutionary routes (not) taken in the recent past among closely-related species may help predict how species will respond to natural and anthropogenic climate change (Kellerman *et al*. 2012; Donovan *et al*. 2014). Finally, crop breeders can take advantage of existing trait variation in crop-wild relatives to develop new varieties for sustainable agriculture (Moyle & Muir 2010; Dennison 2012; Giuliani *et al*. 2013). Hence, if coordination among leaf traits is limited among closely-related species, then broad-scale or global trait spectra may be of little use in addressing fundamental challenges like the ecology of local adaptation (Kawecki & Ebert 2004), near-term responses to climate change, and crop breeding. Conversely, weak coordination may indicate significant opportunities for natural and artificial selection to fine-tune leaf traits in response to different ecological circumstances.

We used a common garden experiment to measure coordination between leaf traits, specifically diffusive and biochemical limitations on photosynthesis and water-use efficiency as well as leaf structure. We considered these traits in relation to climate of origin among tomato species (*Solanum* sect. *Lycopersicon*) and their relatives (*Solanum* sect. *Juglandifolia* and *Lycopersicoides*). These species are closely related herbaceous perennials: fossil-calibrated molecular clocks put section *Lycopersicon* at approximately 2.48 my old, and the split between *Lycopersicon* and *Lycopersicoides* at approximately 4.7 my ago (Särkinen *et al.* 2013). Despite sharing a recent common ancestor, tomato species are ecologically and phenotypically diverse (Moyle 2008; Peralta *et al.* 2008; Nakazato *et al*. 2008, 2012; Chitwood *et al*. 2012; Haak *et al*.

2014; Muir & Thomas-Huebner 2015). Adaptation to different climates, especially along temperature and precipitation gradients, may have played an important role in diversification (Nakazato *et al*. 2010). Most wild tomato species are interfertile (e.g. Baek *et al*. 2015) with the domesticated tomato (*S. lycopersicum* var. *esculentum*), providing a valuable source of germplasm for crop improvement. In particular, altering leaf CO_2 diffusion properties may enhance photosynthetic rate and/or water-use efficiency (Tholen *et al*. 2012; Flexas *et al*. 2013; Gago *et al*. 2014; Buckley & Warren 2014; Flexas *et al*. 2015). Diffusion limits photosynthesis in some wild tomato species (Muir *et al.* 2014) and cultivars (Galmés *et al*. 2011, 2013), but we know little about the ecological and evolutionary significance of this variation.

More generally, we know relatively more about the mechanistic basis of variation in leaf photosynthesis than its ecological or adaptive significance. Stomatal and mesophyll CO_2 diffusion are strongly affected by leaf anatomy (Brown & Escombe 1900; Franks & Farquhar 2001; Nobel 2009; Tholen and Zhu 2011; Tomás *et al*. 2013); biochemical limitations depend on the amount of Rubisco, its activation and catalytic rates (Farquhar *et al*. 1980; von Caemmerer 2000; Galmés *et al*. 2014). Maximum photosynthetic rates are generally higher among certain plant functional types (herbs, C_3 graminoids, and crop plants) than others (trees, sclerophylls, and succulents) (Körner *et al*. 1979; Wullschleger 1993; Flexas *et al*. 2008). These broad-scale correlations suggest that slow growing plants tradeoff high photosynthetic rate in favor of leaf traits that may have other fitness benefits, such as durability, defense against herbivores, or increased resource-use efficiency (Turner 1994; Aerts 1995; Onoda *et al*. 2011).

We found surprisingly weak coordination among CO_2 diffusion, biochemical capacity, photosynthesis, water-use efficiency, and leaf structure among 19 wild and cultivated tomato taxa. The principal axis of variation indicates an expected tradeoff between robust leaf structure

and photosynthesis. However, there was substantial variation orthogonal to this axis that allowed some species simultaneously achieve relatively high photosynthetic rates and intrinsic water-use efficiency. Also, contrary to expectations from the literature, there was no indication that more conservative leaf traits were associated with drier or hotter environments. If anything, there was a signature of less robust leaf structure among species from the driest habitats. Thus, our data suggest that functional trait spectra inferred from global comparisons across plant families and functional types may be of limited utility for predicting short-term evolutionary responses.

Methods

Plant materials and cultivation

We obtained seeds of 19 taxa, 16 wild species (Table S1) from the Tomato Genetics Resource Center at UC Davis (TGRC; http://tgrc.ucdavis.edu) as well as 3 cultivated accessions of *S. lycopersicum* var. *esculentum*, cv. 'Roma VF' (Batlle S.A.) and two Mediterranean 'Tomàtiga de Ramellet' accessions from the University of the Balearic Islands seedbank collection (UIB1-30 and UIB1-48). To even out plant size during measurements, and following TGRC indications, slower growing species were germinated two weeks ahead of faster growing species. Seeds were soaked in 2.5% sodium hypochlorite (household bleach) for 30 or 60 minutes (following TGRC instructions for each species), rinsed thoroughly, and placed on moist paper to germinate. After one week, seedlings were transplanted to cell-pack flats. Two weeks later, five plants of each taxa were transplanted to 19 L pots where the experiment was performed. Pots contained a mixture of standard horticultural substrate mixed with pearlite in a 4:1 proportion v/v. Plants were grown outdoors in an open experimental field under typical Mediterranean conditions at the University of the Balearic Islands (39° 38' 14.9'' N, 2° 38' 51.5'' E) during spring-summer

126 season. Plants were irrigated to field capacity daily to prevent drought stress and fertilized
127 weekly with an NPK solution.
128
129 *Diffusional and biochemical constraints on photosynthesis and water-use efficiency*
130 We measured stomatal (g_s), mesophyll (g_m) conductance to CO_2, net CO_2 assimilation rate (A_N)
131 at ambient CO_2 concentrations, and intrinsic water-use efficiency ($iWUE = A_N / g_{sw}$) using an
132 open-path infrared gas exchange analyzer (LI-6400 or LI-6400XT, LI-COR Inc., Lincoln, NE,
133 USA) with a 2-cm^2 leaf chamber fluorometer. Note that g_s and g_{sw} refer to stomatal conductance
134 to CO_2 and H_2O, respectively. Each leaf acclimatized in the chamber until steady state (usually
135 15-30 min) under standardized conditions: ambient CO_2 (C_a = 400 ppm); constant leaf
136 temperature (T_{leaf} = 25° C), saturating irradiance (photosynthetically active radiation, PAR =
137 1500 µmol quanta m^{-2} s^{-1}), and moderate humidity (relative humidity = 40-60%). We took point
138 measurements of all traits under these steady-state conditions. Additionally, we calculated the
139 maximum rate of carboxylation (V_{cmax}) using A-C_c curves and leaf dark respiration (R_{dark}) at
140 predawn. Estimating g_m can be particularly sensitive to assumed parameter values. To accurately
141 measure g_m we estimated species-specific parameters of leaf respiration, light
142 absorptance/photosystem partitioning, and Rubisco kinetic parameters. Further detail on
143 measuring g_m using combined gas exchange and chlorophyll fluorescence is provided in
144 Methods S1. To investigate Rubisco kinetics, we also sequenced the *rbc*L gene encoding the
145 Rubisco large subunit (LSu) from each species to identify amino acid sequence changes that
146 could alter Rubisco kinetics (see Methods S1 for further detail). Next, we characterized Rubisco
147 kinetic parameters directly from two species (*S. lycopersicum* var. *esculentum*, cv. 'Roma VF'
148 and *S. lycopersicoides*) representing the two Rubisco LSu types identified from sequence

149 analysis (Methods S1). Kinetic properties of the two Rubisco LSu types were compared using
150 ANOVA.
151
152 *Leaf anatomical measurements*
153 We used the youngest, unshaded, fully-expanded leaf from each individual. Leaves were
154 immediately weighed and scanned to obtain fresh mass (FM) and leaf area (LA), respectively.
155 Afterwards, leaves were dried for at least 48 h in a drying oven at 60 °C to obtain dry mass
156 (DM). We report *LMA* (as DM/LA) on whole leaves, which in tomato are pinnately compound,
157 but we excluded structural, non-laminar portions (petiole, rachis, and petioules) because we were
158 particularly interested tradeoffs between leaf structure and diffusive conductance within the
159 lamina. Because leaf thickness measurements using a micrometer are unreliable in tomato leaves
160 (C.D. Muir, pers. obs), we estimated leaf thickness (*LT*) using the method of Vile *et al*. (2005):

$$LT = \frac{LMA}{LDMC} \quad \text{(S1)}$$

161 *LDMC* is the leaf dry matter content, the ratio of leaf DM to saturated FM. Leaf thickness
162 calculated using Eq. 1 is closely correlated with leaf thickness measured from sections in
163 tomatoes (Muir *et al*. 2014). We obtained leaf morphological data from 80 of 82 individuals.
164
165 *Statistical analyses*
166 We used phylogenetic linear mixed effects models (`phyloLME') to estimate key relationships
167 among traits while accounting for phylogenetic nonindependence. Specifically, we fit statistical
168 models using a Bayesian Markov chain Monte Carlo (MCMC) algorithm implemented in the R
169 package MCMCglmm version 2.21 (Hadfield 2010). For all models, we ran the MCMC chain
170 under diffuse priors for 10^6 steps after a burn-in of 10^5 steps, sampling the posterior distribution

10^4 times every 10^2 steps. We tested whether stomatal and mesophyll conductance were significantly correlated with A_N and *iWUE*. These variables were log-transformed for linearity and homoscedasticity. We estimated the effect of these diffusion traits on A_N and *iWUE* from the mode of the posterior distribution and inferred statistical significance if the 95% highest posterior density (HPD) interval did not overlap zero. We simultaneously tested whether phylogeny explained photosynthetic trait variation by including Species as a phylogenetically-structured random effect and compared that to a model without Species using the deviance information criterion (DIC), where a decrease of 2 or more is interpreted as a significant increase in model fit. We used a maximum likelihood phylogenetic tree inferred from 18 genes (Figure 1; Haak *et al.* 2014). Maximum likelihood analyses were conducted using RAxML version 8.1.24 (Stamatakis 2014). The topology of the best tree agreed with previous Bayesian estimates (Rodriguez *et al.* 2009).

We used principal component analysis (PCA) to identify major axes of variation among nine leaf traits: g_m, g_s, A_N, V_{cmax}, R_{dark}, *iWUE*, *LMA*, *LT*, *LDMC*. All traits except V_{cmax} and R_{dark} were log-transformed to make the distribution approximately multivariate normal. Parallel analysis of the trait correlation matrix using the 'parallel' function from the R package nFactors version 2.3.3 (Raiche 2010) indicated that the first four principal components explained significantly more variance, 90.0% cumulatively, than expected by chance from an uncorrelated matrix with rank 7 (we used 9 traits, but *iWUE* and *LT* are linear combinations of other traits). We focus on the first principal component, denoted PC1, which explained a moderate amount of variation (35.5%). For reference, PC1 loaded positively with leaf thickness and *LMA*, but negatively with A_N and components of CO_2 diffusion (g_m, g_s).

193 To test the hypothesis that species from dry and/or hot environments tradeoff efficient
194 CO_2 diffusion for a more robust, stress-tolerant leaf anatomy, we looked at the correlation
195 between mean annual precipitation and temperature to species' average position along PC1. For
196 this analysis, we removed the three cultivars of *S. lycopersicum* var. *esculentum* and one
197 accession *S. lycoperiscum* var. *cerasiforme*, an unimproved landrace. To reduce the influence of
198 a single outlier species (*S. juglandifolium*), we shrank the interspecific variance of PC1 using a
199 signed logarithm transformation:

$$\mathrm{PC1}_T = \mathrm{sign}(\mathrm{PC1})\ \log|\mathrm{PC1}| \qquad \text{(S2)}$$

200 We also performed analyses with and without this species. We obtained mean annual
201 precipitation and temperature at the habitat of origin for each source population from Worldclim
202 (Hijmans *et al.* 2005), which has been used previously to study climatic adaptation in wild
203 tomatoes (Chitwood *et al.* 2012; Nakazato *et al*. 2008). Phylogenetic regression was carried out
204 with the R package phylolm version 2.2 (Ho & Ané 2014) using the 'OUrandomRoot' model to
205 account for phylogenetic nonindependence. Other trait-climate relationships were tested in the
206 same way.
207
208 **Results**
209 *CO_2 diffusion and biochemistry limit photosynthesis and alter water-use efficiency*
210 Tomato species vary considerably in photosynthetic rate (A_N) and intrinsic water-use efficiency
211 (*iWUE*), driven by constraints on leaf CO_2 diffusion and the maximum rate of carboxylation
212 (V_{cmax}). Phylogenetic linear mixed effects models (`phyloLME') showed that between individual
213 plants, stomatal (g_s) and mesophyll (g_m) conductance increased A_N (Table 1; Figure 2A,B), but
214 had opposing effects on *iWUE* (Table 1). However, phylogenetic relationship explained little of

the trait variation, thus phylogenetic and nonphygenetic gave nearly identical results (Table 1). Increased g_s was associated with lower *iWUE* (Figure 2C), whereas greater g_m was associated with greater *iWUE* (Figure 2D). Like g_m, greater biochemical capacity, as indicated by V_{cmax}, was associated with significantly greater A_N and *iWUE* (Figure 2). Thus, species achieved high photosynthetic rates via two routes: high g_s, but lower *iWUE* or high g_m, but relatively high *iWUE*. The drawdown of CO_2 concentration from the leaf interior (C_i) to the chloroplast (C_c), another indicator of diffusional constraint in the leaf mesophyll, was even more strongly correlated with *iWUE* than g_m (Figure S1), arguing that reduced internal diffusion enhances *iWUE*.

Limited variation in Rubisco biochemistry between tomato species

The two Rubisco LSu types showed significant differences in some of the kinetic parameters (Table 2; see Methods S1 for description of how types were identified and Results S1 for further detail on molecular evolution of *rbc*L in tomatoes). Interestingly, the Rubisco LSu type 2, which occurred in the domesticated clade species (*S. pimpinellifolium*, *S. cheesmaniae*, *S. galapagense*, *S. lycopersicum* var. *cerasiforme*, and the cultivars; see Figure S2) and *S. habrochaites*, had a higher $S_{c/o}$ value, which was due to higher Michaelis-Menten constant for CO_2 under atmospheric conditions (K_c^{air}) and lower catalytic turnover rate for the oxygenase reaction (k_{cat}^{o}) compared to the Rubisco LSu type 1. Non-significant differences were observed between the two Rubisco LSu types in the remaining kinetic parameters.

Modest coordination between leaf physiological and structural traits

237 The first principal component (PC1) accounted for 35.5% of the variation among individual leaf
238 physiology (g_m, g_s, A_N, V_{cmax}, R_{dark}, *iWUE*) and bulk anatomy (*LMA*, *LT, LDMC*). On one end of
239 this axis were thin leaves with fast CO_2 diffusion and high A_N; on the other were thick leaves
240 with slower CO_2 diffusion and lower A_N (Figure 3). This principal component indicates an axis
241 of leaf trait variation likely mediated by tradeoffs between more robust leaf structure (i.e. higher
242 *LMA* and *LT*) and CO_2 diffusion. However, the modest amount of trait variance explained
243 indicates that this tradeoff does not tightly constrain leaf trait evolution in tomatoes. The second
244 principal component (PC2; 23.8% variance explained) was most strongly associated with *iWUE*
245 and showed that greater *iWUE* was associated with higher water content (lower *LDMC*) leaves
246 (Figure 3).
247
248 *Limited evidence leaf trait-climate associations*
249 Contrary to the hypothesis that dry, hot environments select for a stress-tolerant, robust leaf
250 structure, thinner leaves and more rapid CO_2 diffusion (i.e. higher values of PC1) was associated
251 with drier habitats (PC1-Precip, $P = 0.012$), but not temperature (PC1-Temp, $P = 0.069$).
252 However, this correlation between PC1 and precipitation was strongly influenced by a single
253 species, *S. juglandifolium* (Figure 4), and was not significant if this species was removed (PC1-
254 Precip, $P = 0.266$). Certain traits that loaded strongly with PC1, especially *LMA* and *LT*, were
255 strongly associated with precipitation. Specifically, species from the driest habitats had the
256 thinnest leaves, even when *S. juglandifolium* was excluded (Figure S3). Our data therefore do not
257 support the hypothesis that species tradeoff slow CO_2 diffusion and lower metabolic rates for
258 robust leaf structure in stressful environments. All trends in the data are actually in the exact
259 opposite direction.

Discussion

Many ecologists seek to distill organismal variation down to a manageable number of key functional traits (e.g. Perez-Harguindeguy *et al*. 2013). Leaf traits in particular, which are necessarily constrained by the need to capture sunlight, CO_2, and manage nutrient/water, may fall along a single 'fast-slow' continuum (Reich 2014 and references therein) associated with resource acquisitive and resource conservative traits (Mason & Donovan 2015). The key assumptions are that leaf structural traits such as leaf mass per area (*LMA*) strongly constrain photosynthesis by reducing CO_2 diffusion and that there is strong selection for tight coordination between CO_2 diffusion and biochemical capacity for photosynthesis. These assumptions have been evaluated at broad phylogenetic scales, but rarely addressed among closely-related species. This is important because patterns among distantly related species can be driven primarily by disparate functional groups (e.g. deciduous versus evergreen species) that have little bearing on the incremental evolutionary steps taken as species adapt to new environments.

In tomatoes, we found evidence for a 'fast-slow' spectrum mediated by diffusional/biochemical constraints and leaf structure, but this spectrum explained a modest amount of total leaf trait variation. There is no precise prediction for exactly how much coordination we *should* have seen under the coordination hypothesis, but variation was well-distributed across the first four components, indicating multiple important axes. Furthermore, although thicker leaves with greater *LMA* were associated with reduced CO_2 diffusion, the relationships were weak (Figure S4), demonstrating ample scope for thick and/or dense leaves to have relatively high diffusion and *vice versa*. Finally, lack of coordination cannot be explained by relatively little physiological variation between species. Indeed, despite sharing a recent

283 common ancestor, we observed a dramatic range in traits like A_N (6.4 – 33.0 μmol CO_2 m^{-2} s^{-1}) in
284 wild tomatoes. In fact, our study should have been especially able to detect coordination, if it
285 existed, because we measured plants with similar growth form and functional type in a common
286 garden at the same age, eliminating sources of variation common in other studies. The lack of
287 tight coordination between leaf structure, CO_2 diffusion, and photosynthetic biochemistry means
288 there may be multiple, loosely coordinated axes of leaf trait variation that provide a substrate for
289 labile, unconstrained evolution in response to novel selective pressures from climate change and
290 crop breeders.

291 In fact, many combinations of stomatal conductance (g_s), mesophyll conductance (g_m),
292 and V_{cmax} resulted in similar photosynthetic rates but very different water-use efficiencies (Figure
293 2). Typically, we expect that to increase photosynthetic rate, plants must increase stomatal
294 conductance, increasing transpirational loss and decreasing water-use efficiency. If mesophyll
295 conductance and biochemical capacity were closely coordinated with stomatal conductance, then
296 there would be limited opportunity to increase water-use efficiency without sacrificing
297 photosynthetic rate. However, we find that there may be substantial scope to increase
298 photosynthetic rate while maintaining high water-use efficiency. Indeed, photosynthetic rate and
299 water-use efficiency were essentially uncorrelated. This axis of variation was evident in a second
300 principal component that loaded positively with *iWUE* but was orthogonal to A_N (Figure 3). Why
301 don't all species have high photosynthetic rate and water-use efficiency? In nature, there are
302 probably other tradeoffs, especially nitrogen limitation, that prevent species from having greater
303 mesophyll conductance and/or V_{cmax}.

304 Photosynthetic variation in tomatoes is primarily mediated by anatomical differences in
305 leaves rather than differences in Rubisco kinetics. In contrast to other clades of C_3 plants that

306 have undergone rapid diversification into different environments, evolutionary changes in
307 Rubisco kinetics (e.g. faster rates of carboxylation or greater affinity for CO_2 over O_2) do not
308 appear to play a major role in the evolution of tomatoes. This contrasts with other plant groups
309 like *Limonium* (Galmés *et al.* 2014), which underwent adaptive evolution of Rubisco kinetics
310 during their radiations into novel environments. Future work is needed to understand why some
311 clades respond to selection through changes in protein biochemistry, whereas groups like tomato
312 seem to primarily differ in anatomical traits.

313 We also find no evidence that drier or hotter environments favor robust leaf structure or
314 'slow', resource conservative strategies (low conductance, low V_{cmax}) in wild tomatoes (Figure
315 4). Obviously, our study does not have the statistical power of broad comparative analyses (e.g.
316 Wright *et al*. 2005), but the trends in the data were not even in the predicted direction. If
317 anything, there was a tendency for species from the driest habitats to be on the 'fast' end of the
318 leaf trait spectrum (see also Easlon & Richards 2009), but this was largely influenced by a single
319 species, *S. juglandifolium*. Thus, tomato species in dry habitats may rely primarily on a form of
320 drought tolerance, growing fast when water is available and dying back or going dormant during
321 droughts. Alternatively, leaf traits may be decoupled from other traits (e.g. root:shoot ratios) that
322 confer alternative drought avoidance or tolerance mechanisms.

323 The modest coordination we observe between leaf structure and physiological function
324 indicates that bulk structural traits like leaf mass per area are probably insufficient to identify the
325 most important axes of trait variation (Figure S4). Traits like leaf thickness and leaf mass per
326 area are probably important in setting the upper bounds on maximum potential CO_2 diffusion and
327 photosynthetic rate (Flexas *et al*. 2008), but realized values depend on the precise anatomical and
328 biochemical features of the leaf that are not well-captured by bulk structural traits (Tosens *et al*.

329 2012; Tomás *et al*. 2013). This suggests the possibility that there are many unique axes that vary
330 leaf anatomy and photosynthesis without large effects on traits like *LMA*. Each of these axes may
331 be a different tradeoff that could be evolutionarily important in some taxa, but not others.

332 From the modest coordination between leaf structure and function in wild tomatoes, we
333 can make three major conclusions:

334 1. The leaf functional traits most commonly used comparative ecology (e.g. *LMA*) may not be
335 good proxies for leaf function, especially among closely-related species. This is not because
336 there was little variation among tomatoes. Tomato leaves varied widely in diffusional,
337 biochemical, and structural traits, but there was remarkably little covariation between bulk
338 structure and function.
339 2. Hence, broad-scale patterns of functional trait covariation may not be useful in predicting
340 adaptive evolution in the recent past or in response to climate change. Nor should we expect
341 that the relationship between traits and environments observed at broad phylogenetic scales
342 (e.g. thick leaves in hot, dry environments) will hold at smaller scales. If anything, we found
343 that low-*LMA*, resource acquisitive traits were associated with dry environments, the
344 opposite of what is commonly predicted (see also Mason & Donovan 2015).
345 3. Although our study challenges commonly-held assumptions about the relationships between
346 leaf structure and function, this does not refute that intimate structure-function relationships
347 exist. Rather, detailed anatomical traits such as guard cell dimensions, mesophyll structure,
348 and photochemical enzyme concentrations are needed to identify the most important
349 tradeoffs defining leaf anatomy and physiology.

Adaptive radiation of tomatoes and other plant groups undoubtedly requires evolution of new morphological and physiological traits, but this study suggests that we do not yet have a general explanation for variation in the most important leaf traits affecting photosynthesis.

Acknowledgements

CDM was supported by an Evo-Devo-Eco Network (EDEN) research exchange (NSF IOS #0955517). The research was supported by project AGL2013-42364-R (Plan Nacional, Spain) awarded to JG. We acknowledge Trinidad García at the radioisotope service (UIB), and Miquel Truyols and collaborators of the UIB Experimental Field and Greenhouses for their technical support. Chase Mason provided feedback.

References

Aerts, R. (1995). The advantages of being evergreen. *TREE,* 10, 402-407.

Baek, Y. S.. *et al.* (2015). Testing the SI× SC rule: Pollen–pistil interactions in interspecific crosses between members of the tomato clade (*Solanum* section *Lycopersicon*, Solanaceae). *Am. J. Bot*., 102, 302-311.

Brown, H. T. & F. Escombe. (1900). Static diffusion of gases and liquids in relation to the assimilation of carbon and translocation in plants." *Proceedings of the Royal Society of London,* 67, 124-128.

Buckley, T. N. *et al*. (2014). The role of mesophyll conductance in the economics of nitrogen and water use in photosynthesis. *Photosynthesis research,* 119, 77-88.

Chave, J. *et al.* (2009). Towards a worldwide wood economic spectrum. *Ecol. Lett.*, 12, 351–366.

Chitwood, D. H. *et al.* (2012). Native environment modulates leaf size and response to simulated

foliar shade across wild tomato species. *PLoS ONE,* 7:e29570. doi:10.1371/journal.pone.0029570.

Donovan, L.A., *et al.* (2014). Ecological and evolutionary lability of plant traits affecting carbon and nutrient cycling. *J. Ecol.,* 102, 302-314.

Denison, R. F. (2012). *Darwinian agriculture: how understanding evolution can improve agriculture.* Princeton University Press.

Easlon, H. M. & J.H. Richards. (2009). Drought response in self-compatible species of tomato (Solanaceae)." *American Journal of Botany,* 96, 605-611.

Edwards, E. J. *et al*. (2014). Leaf life span and the leaf economic spectrum in the context of whole plant architecture. *J. Ecol.,* 102, 328–336.

Evans, J. R. *et al*. (2009). Resistances along the CO_2 diffusion pathway inside leaves. *J. Exp. Bot.*, 60, 2235-2248.

Farquhar, G. D. *et al.* (1980). A biochemical model of photosynthetic CO2 assimilation in leaves of C3 species. *Planta* 149, 78-90.

Farquhar, G. D. *et al*. (1982). Stomatal conductance and photosynthesis. *Annu Rev. Plant Physiol.*, 33, 317-345.

Flexas, J. *et al*. (2013) Leaf mesophyll conductance and leaf hydraulic conductance: an introduction to their measurement and coordination. *J. Exp. Bot.,* 64, 3965-3981.

Flexas, J., *et al.* (2015). Mesophyll conductance to CO_2 and Rubisco as targets for improving intrinsic water use efficiency in C_3 plants. *Plant Cell Environ.* doi: 10.1111/pce.12622.

Flexas, J. *et al.* (2008). Mesophyll conductance to CO_2: current knowledge and future prospects. *Plant Cell Environ.,* 31, 602-621.

Franks, P.J. & G.D. Farquhar. (2001). The effect of exogenous abscisic acid on stomatal

development, stomatal mechanics, and leaf gas exchange in *Tradescantia virginiana*. *Plant Physiology,* 125, 935-942.

Funk, J. L. *et al*. (2013). Leaf traits within communities: context may affect the mapping of traits to function. *Ecology,* 94, 1893-1897.

Gago, J. *et al.* (2014). Opportunities for improving leaf water use efficiency under climate change conditions. *Plant Science* 226, 108-119.

Galmés, J. *et al.* (2011). Physiological and morphological adaptations in relation to water use efficiency in Mediterranean accessions of *Solanum lycopersicum*. *Plant Cell Environ.,* 34, 245-260.

Galmés J. *et al.* (2013). Leaf responses to drought stress in Mediterranean accessions of *Solanum lycopersicum*: anatomical adaptations in relation to gas exchange parameters. *Plant Cell Environ.,* 36, 920–935.

Galmés, J. *et al.* (2014). Environmentally driven evolution of Rubisco and improved photosynthesis and growth within the C_3 genus *Limonium* (Plumbaginaceae). *New Phyto.,* 203, 989-999.

Giuliani, R. *et al.* (2013). Coordination of leaf photosynthesis, transpiration, and structural traits in rice and wild relatives (genus *Oryza*). *Plant Physiol.,* 162, 1632-1651.

Givnish, T. J. (1986). Optimal stomatal conductance, allocation of energy between leaves and roots, and the marginal cost of transpiration. In: *On the economy of plant form and function* (ed. Givnish, T.J.). Cambridge University Press, 171-213

Grime, J. P. (1977). Evidence for the existence of three primary strategies in plants and its relevance to ecological and evolutionary theory. *Am. Nat.,* 111, 1169-1194.

Haak, D. C. *et al.* (2014). No evidence for phylogenetic constraint on natural defense evolution

among wild tomatoes. *Ecology,* 95,1633–1641.

Hadfield, J.D. (2010). MCMC methods for multi-response generalized linear mixed models: The MCMCglmm R Package. *J. Stat. Soft.*, 33, 1-22.

Hijmans, R. J., S. E. Cameron, J. L. Parra, P. G. Jones, and A. Jarvis. (2005). Very high resolution interpolated climate surfaces for global land areas. *International Journal of Climatology,* 25, 1965-1978.

Ho, L. S. T. & Ane, C. (2014) A linear-time algorithm for Gaussian and non-Gaussian trait evolution models. *Syst. Biol.*, 63, 397-408.

Kawecki, T.J. & D. Ebert. (2004). Conceptual issues in local adaptation. *Ecol. Lett.*, 7, 1225-1241.

Kellermann, V. *et al.* (2012). Upper thermal limits of *Drosophila* are linked to species distributions and strongly constrained phylogenetically. *Proc. Natl. Acad. Sci. U.S.A.,* 109, 16228-16233.

Mason, C. M. & L.A. Donovan. (2015). Evolution of the leaf economics spectrum in herbs: Evidence from environmental divergences in leaf physiology across *Helianthus* (Asteraceae). *Evolution,* 69, 2705-2720.

Medrano, H. *et al.* (2009). Variability in water use efficiency at the leaf level among Mediterranean plants with different growth forms. *Plant and Soil,* 317, 17-29.

Moyle, L. C. (2008). Ecological and evolutionary genomics in the wild tomatoes (*Solanum* sect. *Lycopersicon*). *Evolution,* 62, 2995-3013.

Moyle, L. C. *et al.* (2010). Reciprocal insights into adaptation from agricultural and evolutionary studies in tomato. *Evol. App.,* 3, 409-421.

441 Muir, C. D. *et al*. (2015). Constraint around Quarter-Power Allometric Scaling in Wild Tomatoes
442 (*Solanum* sect. *Lycopersicon*; Solanaceae). *Am. Nat.,* 186, 421-433.
443 Muir, C. D. *et al*. (2014). Morphological and anatomical determinants of mesophyll conductance
444 in wild relatives of tomato (*Solanum* sect. *Lycopersicon*, sect. Lycopersicoides;
445 Solanaceae). *Plant Cell Environ.,* 37, 1415-1426.
446 Nakazato, T. *et al*. (2008). Environmental factors predict adaptive phenotypic differentiation
447 within and between two wild Andean tomatoes. *Evolution,* 62, 774–792.
448 Nobel P.S. (2009) *Physicochemical and Environmental Plant Physiology* 4th edn. Academic
449 Press, London, UK.
450 Ogburn R. M. & E.J. Edwards (2010). The Ecological Water-Use Strategies of Succulent Plants.
451 *Adv. Bot. Res.,* 55, 179-225.
452 Onoda, Y. *et al*. (2011). Global patterns of leaf mechanical properties. *Ecol. Lett.,* 14, 301-312.
453 Parkhurst, D. F. (1994). Diffusion of CO_2 and other gases inside leaves. *New Phyto.,* 126, 449-
454 479.
455 Peralta, I. E. *et al.* (2008). The taxonomy of tomatoes: a revision of wild tomatoes (*Solanum*
456 section *Lycopersicon*) and their outgroup relatives in sections *Juglandifolium* and
457 *Lycopersicoides*. *Syst. Bot. Monogr.,* 84, 1-186.
458 Perez-Harguindeguy, N. *et al.* (2013). New handbook for standardized measurement of plant
459 functional traits worldwide. *Australian Journal of Botany*. 61, 167-234.
460 Pigliucci, M. *et al*. (2003). Phenotypic integration: studying the ecology and evolution of
461 complex phenotypes. *Ecol. Lett.,* 6, 265-272.
462 Raiche, G. (2010). nFactors: an R package for parallel analysis and nongraphical solutions to the
463 Cattell scree test. R package version 2.3.3.

464 Reich, P. B. (2014). The world-wide 'fast-slow' plant economics spectrum: a traits manifesto. *J.*
465 *Ecol.*, 102, 275-301.
466 Sack L. *et al.* (2003). The 'hydrology' of leaves: co-ordination of structure and function in
467 temperate woody species. *Plant Cell Environ.,* 26, 1343–1356.
468 Särkinen, T. *et al.* (2013). A phylogenetic framework for evolutionary study of the nightshades
469 (Solanaceae): a dated 1000-tip tree. *BMC Evol. Biol.,* 13, 214.
470 Tholen, D. *et al*. (2012). Opinion: Prospects for improving photosynthesis by altering leaf
471 anatomy. *Plant Sci.,* 197, 92-101.
472 Tholen, D. *et al.* (2011). The mechanistic basis of internal conductance: a theoretical analysis of
473 mesophyll cell photosynthesis and CO2 diffusion. *Plant Physiol.,* 156, 90-105.
474 Tomás, M. *et al.* (2013). Importance of leaf anatomy in determining mesophyll diffusion
475 conductance to CO_2 across species: quantitative limitations and scaling up by models. *J.*
476 *Exp. Bot.,* 64, 2269-2281.
477 Tosens, T., Ü. Niinemets, V. Vislap, H. Eichelmann & P. C. Díez. (2012) Developmental
478 changes in mesophyll diffusion conductance and photosynthetic capacity under different
479 light and water availabilities in *Populus tremula*: how structure constrains function.
480 *Plant, Cell & Environment,* 35, 839–856.
481 Turner, I.M. (1994). Scleophylly: primariliy protective? *Funct. Ecol.,* 8, 669-675.
482 Vile, D., E. Garnier, B. Shipley, G. Laurent, M.-L. Navas *et al*., (2005) Specific leaf area and dry
483 matter content estimate thicknessin laminar leaves. *Ann. Bot.*, 96, 1129–1136.
484 von Caemmerer, S. (2000). *Biochemical models of leaf photosynthesis*. CSIRO Publishing,
485 Collingwood, Australia.

Westoby, M. *et al*. (2002). Plant ecological strategies: Some leading dimensions of variation 652 between species. *Annu. Rev. Ecol. Syst.,* 33, 125–159.

Wright, I. J. *et al.* (2004). The worldwide leaf economics spectrum. *Nature,* 428, 821-827.

Wullschleger, S. D. (1993). Biochemical limitations to carbon assimilation in C_3 plants—a retrospective analysis of the A/Ci curves from 109 species. *J. Exp. Bot.,* 44, 907-920.

Table 1: Diffusional and biochemical constraints drive variation in photosynthetic rate (A_N) and intrinsic water-use efficiency (*iWUE*) among tomato species. For both A_N and *iWUE*, phylogenetic linear mixed effects models including 'Species' as a random effect improved model fit (lower Deviance Information Criterion [DIC]) over nonphylogenetic linear models, indicating some effect of phylogenetic relatedness. Greater stomatal (g_s) and mesophyll (g_m) conductance significantly increased A_N but had opposing effects on *iWUE*. Likewise, greater maximum carboxylation rates (V_{cmax}) increased both A_N and *iWUE*. Parameters were estimated from the mode of 10^4 samples drawn from the posterior distribution using MCMCglmm. The effects of g_s, g_m, and V_{cmax} are highly significant (95% high posterior density [HPD] intervals do not overlap zero) in all models.

Response Variable	Fixed Effects	Random Effects	DIC	Parameter estimate		95% HPD Interval
$\log(A_N)$	$\log(g_s)$	(none)	-233.4	$\log(g_s)$	0.39	0.35 – 0.43
	$\log(g_m)$			$\log(g_m)$	0.31	0.28 – 0.34
	V_{cmax}			V_{cmax}	9.7×10^{-3}	$7.2 – 12.5 \times 10^{-3}$
	$\log(g_s)$	Species	-250.5	$\log(g_s)$	0.36	0.32 – 0.40
	$\log(g_m)$			$\log(g_m)$	0.32	0.28 – 0.35
	V_{cmax}			V_{cmax}	9.2×10^{-3}	$6.4 – 12.0 \times 10^{-3}$
$\log(iWUE)$	$\log(g_s)$	(none)	-233.1	$\log(g_s)$	-0.61	-0.64 – -0.57
	$\log(g_m)$			$\log(g_m)$	0.31	0.28 – 0.34
	V_{cmax}			V_{cmax}	9.7×10^{-3}	$7.1 – 12.3 \times 10^{-3}$
	$\log(g_s)$	Species	-250.5	$\log(g_s)$	-0.64	-0.67 – -0.60
	$\log(g_m)$			$\log(g_m)$	0.32	0.28 – 0.35

V_{cmax}	V_{cmax}	9.2×10^{-3}	$6.3 – 12.0 \times 10^{-3}$

Table 2. Comparison of the Rubisco kinetics at 25ºC for the two Rubisco LSu types detected among wild and domesticated tomatoes based on the amino acid sequence, namely LSu types 1 and 2. Parameters, measured in a representative species of each Rubisco type, describe the Michaelis-Menten constant for CO_2 under 0% O_2 (K_c) and 21% O_2 (K_c^{air}), the maximum rates of carboxylation (k_{cat}^c) and oxygenation (k_{cat}^o), carboxylation catalytic efficiency (k_{cat}^c/K_c), and specificity factor ($S_{c/o}$). Data are means ± SE of four replicates per Rubisco type. Significant differences between both Rubisco types are indicated by the ANOVA *P*-value, * <0.05; ** <0.01.

Rubisco LSu type	1	2	*P* value
Species measured	*S. lycopersicoides*	*S. lycopersicum*	
K_c (mM)	9.3 ± 0.9	8.2 ± 0. 7	0.308
K_c^{air} (mM)	16.6 ± 0.8	13.5 ± 0.8	0.020*
k_{cat}^c (s^{-1})	2.430 ± 0.138	3.142 ± 0.518	0.176
k_{cat}^o (s^{-1})	0.892 ± 0.099	1.359 ± 0.108	0.010**
k_{cat}^c/K_c (s^{-1} mM^{-1})	0.261 ± 0.026	0.391 ± 0.075	0.127
$S_{c/o}$ (mol mol^{-1})	99.4 ± 3.5	115.0 ± 2.1	0.007**

514 **Figures**

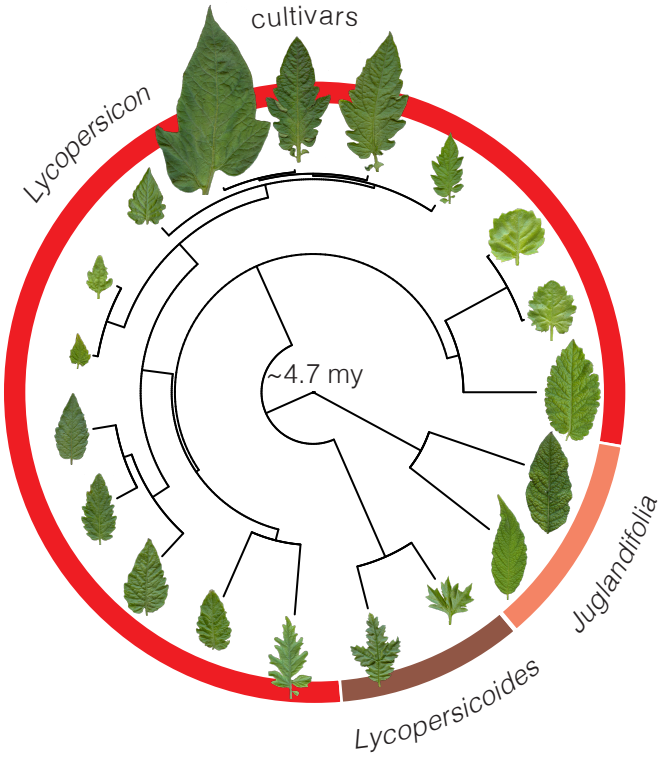

515

516 **Figure 1**: Wild tomatoes and cultivars are closely-related, yet phenotypically-diverse taxa.
517 Among species investigated here, the oldest split is approximately 4.7 my based on a fossil-
518 calibrated phylogeny (Särkinen *et al*. 2013). Functional traits like terminal leaflet size, depicted
519 for each species at the tips of the phylogeny, as well as leaf physiological and structural traits
520 used in this study vary widely among species.

521

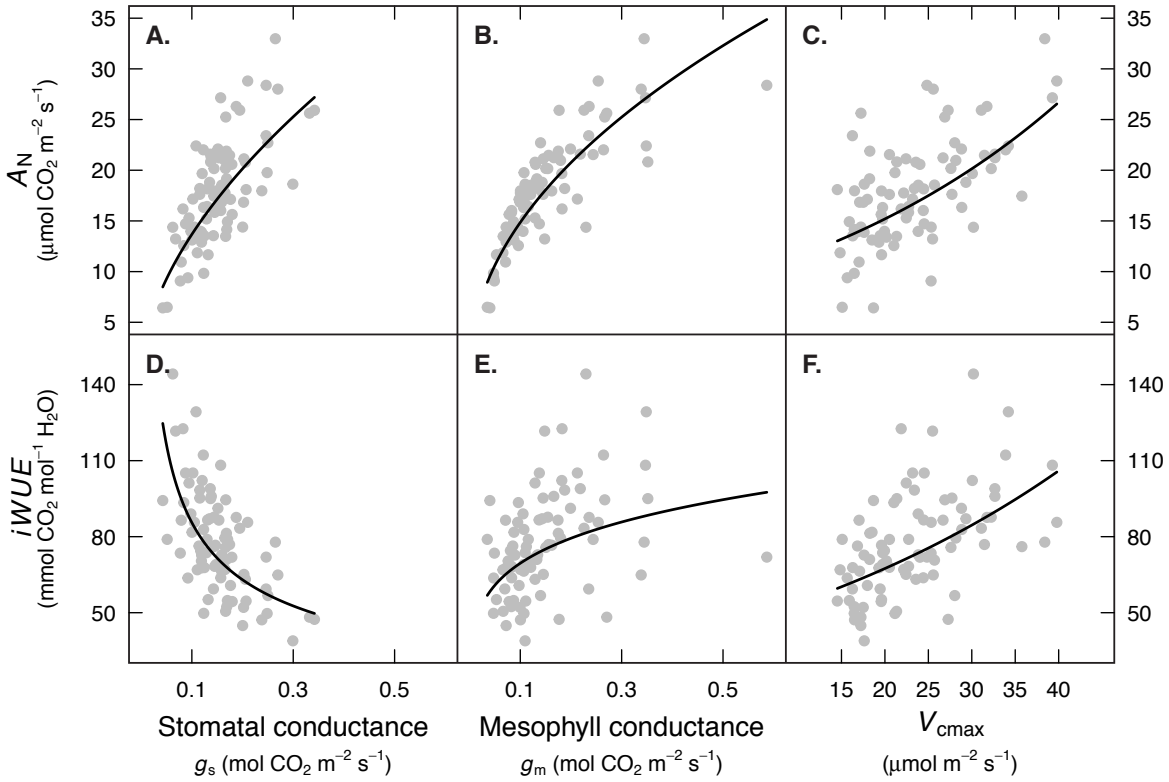

Figure 2: Leaf CO_2 diffusion and biochemistry limit net CO_2 assimilation rates (A_N) and alter intrinsic water-use efficiency (*iWUE*). Each point is data from one of 82 individual plants across 19 wild and cultivated tomato taxa. Panels A. and B. show that faster diffusion through stomata (g_s) and mesophyll (g_m) resulted in higher A_N. However, these parameters had opposing effects on *iWUE*. Greater g_s lowered *iWUE* (panel D.), whereas greater g_m increased *iWUE* (panel E.). Leaf biochemistry, specifically the maximum rate of carboxylation (V_{cmax}) also increased A_N (panel C.) and *iWUE* (panel F.). Fitted lines are based on a Bayesian phylogenetic mixed models treating Species as a random effect: $\log(A_N) \sim \log(g_s) + \log(g_m) + V_{cmax} + (1|\text{Species})$ and $\log(iWUE) \sim \log(g_s) + \log(g_m) + V_{cmax} + (1|\text{Species})$. For visual aid, lines were drawn to account for positive covariation between g_s, g_m, and V_{cmax} (data not shown). For example, panel

533 A. shows the predicted A_N at a given g_s with g_m and V_{cmax} set to the predicted value at a given g_s.

534 All slopes were significantly different than zero ($P < 0.0001$) based on 10^4 MCMC samples from

535 the posterior distribution of the model.

536

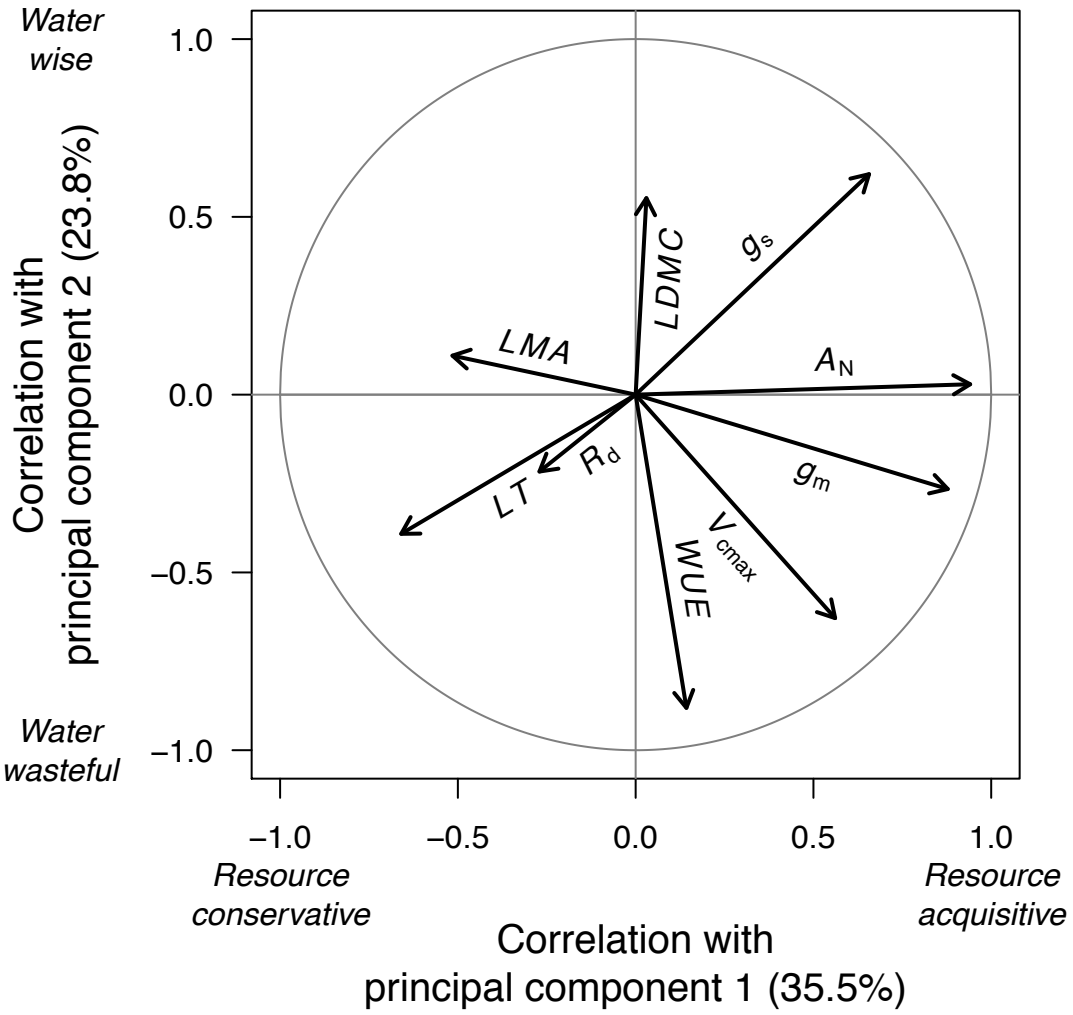

537

538 **Figure 3**: Major axes of leaf trait variation in tomato. The first axis, principal component 1,
539 explains 35.5% of the total variation. It delineates plants along a continuum from resource
540 acquisitive (higher PC1, greater A_N, thinner leaves) to resource conservative (lower PC1, lower
541 A_N, thicker leaves). The second axis, principal component 2, explains 23.8% of the trait variation
542 and delineates an axis from more water wise (higher PC2, greater *iWUE*) to water wasteful
543 (lower PC2, lower *iWUE*). The arrows are vectors showing the correlation across individual
544 plants between a trait and both principal components. For example, A_N is positively correlated

545 with PC1, but uncorrelated with PC2. The grey circle shows the outer possible set of correlation
546 combinations. Abbreviations: R_{dark} = dark respiration rate; *iWUE* = intrinsic water-use efficiency;
547 V_{cmax} = maximum rate of carboxylation; g_m = mesophyll conductance; A_N = net CO_2 assimilation
548 rate; g_s = stomatal conductance; *LDMC* = leaf dry matter content; *LMA* = leaf mass per area; *LT*
549 = leaf thickness.
550

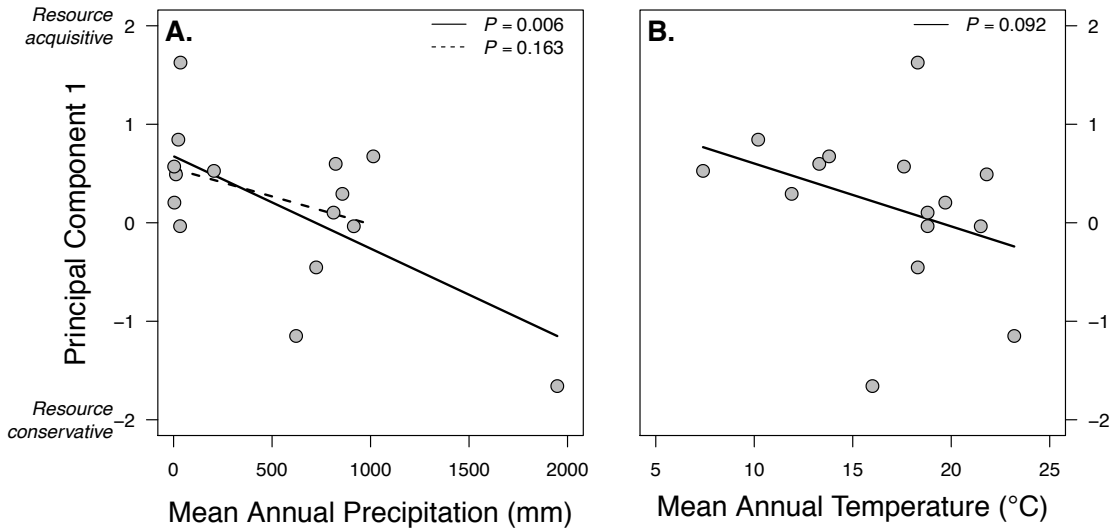

551

552 **Figure 4**: The resource conservative to acquisitive axis of leaf trait variation was uncorrelated
553 with mean annual precipitation (A.) and temperature (B.). Each point shows the climate at
554 habitat of origin for a different wild tomato taxon and its position, averaged from multiple
555 individuals in the experiment, along the resource acquisitive to conservative axis. There was a
556 significant positive correlation between PC1 and precipitation, but this was driven by a single
557 influential species, *S. juglandifolium*; the correlation was not significant once this species was
558 removed. All *P*-values are from phylogenetic linear regression.

559

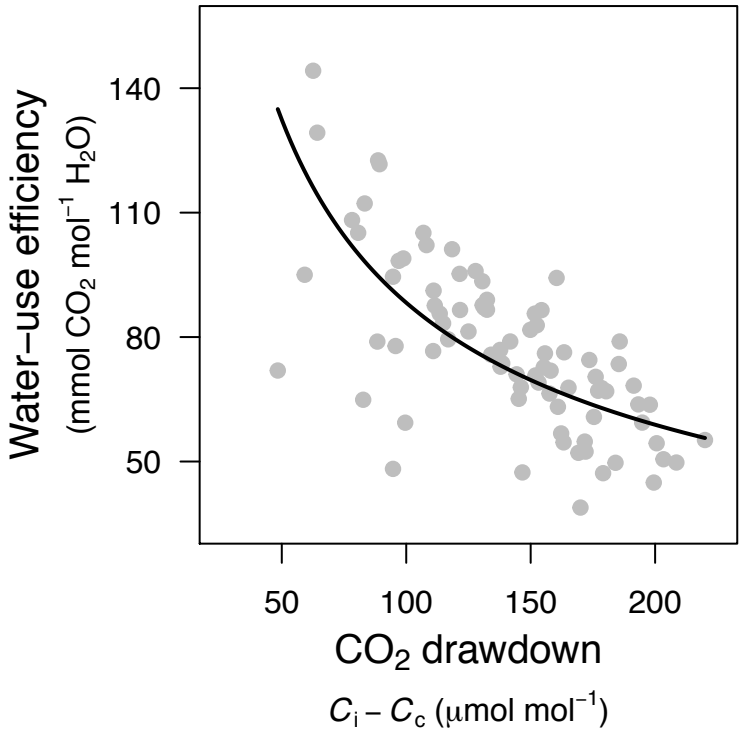

560

561 **Figure S1:** CO_2 drawdown from the leaf interior (C_i) to the chloroplast (C_c) is negatively

562 associated with i*WUE* in tomatoes, indicating that reduced diffusional constraints (lower $C_i - C_c$)

563 leads to increased *iWUE*. Fitted line is based on a Bayesian phylogenetic mixed models treating

564 Species as a random effect: $\log(iWUE) \sim \log(C_i - C_c) + (1|\text{Species})$. The slope is significantly

565 different than zero ($P < 0.0001$) based on 10^4 MCMC samples from the posterior distribution of

566 the model.

567

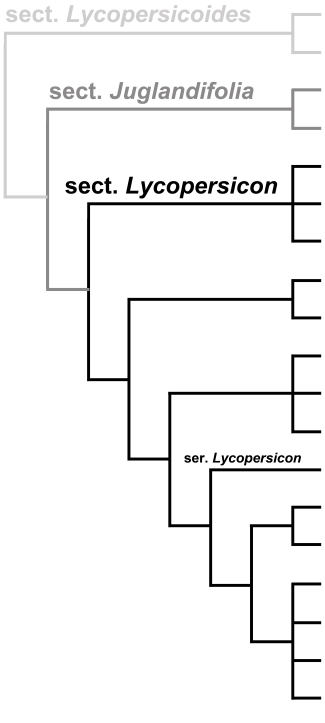

Taxon	Nucleotide						Amino acid	
	81	255	573	688	822	Haplotype	230	LSu type
S. lycopersicoides	T	C	A	G	C	1	A	1
S. sitiens	T	C	A	G	C	1	A	1
S. ochranthum	G	T	A	G	C	2	A	1
S. juglandifolium	G	T	G	G	C	3	A	1
S. pennellii	T	C	A	G	C	1	A	1
S. pennellii var. *puberulum*	T	C	A	G	C	1	A	1
S. habrochaites	T	C	A	A	C	5	T	2
S. chilense	T	C	A	G	C	1	A	1
S. peruvianum	T	C	A	G	C	1	A	1
S. arcanum	T	C	A	G	C	1	A	1
S. neorickii	T	C	A	G	C	1	A	1
S. chmielewskii	T	C	A	G	C	1	A	1
S. pimpinellifolium	T	C	A	A	T	4	T	2
S. cheesmaniae	T	C	A	A	T	4	T	2
S. galapagense	T	C	A	A	T	4	T	2
S. lycopersicum var. *cerasiforme*	T	C	A	A	T	4	T	2
Ramellet tomato 1-48	T	C	A	A	T	4	T	2
Ramellet tomato 1-30	T	C	A	A	T	4	T	2
Commercial tomato 'Roma VF'	T	C	A	A	T	4	T	2

Figure S2: Evolutionary patterns of the Rubisco large subunit (LSu) among wild and domesticated tomato species. The species relationships shown are based on an 18-gene phylogeny from Haak *et al*. (2014; see Methods). Nucleotide differences in the *rbc*L gene are indicated, giving rise to five different haplotypes. Those mutations result in a single difference at amino acid level and thus two Rubisco LSu types within tomatoes.

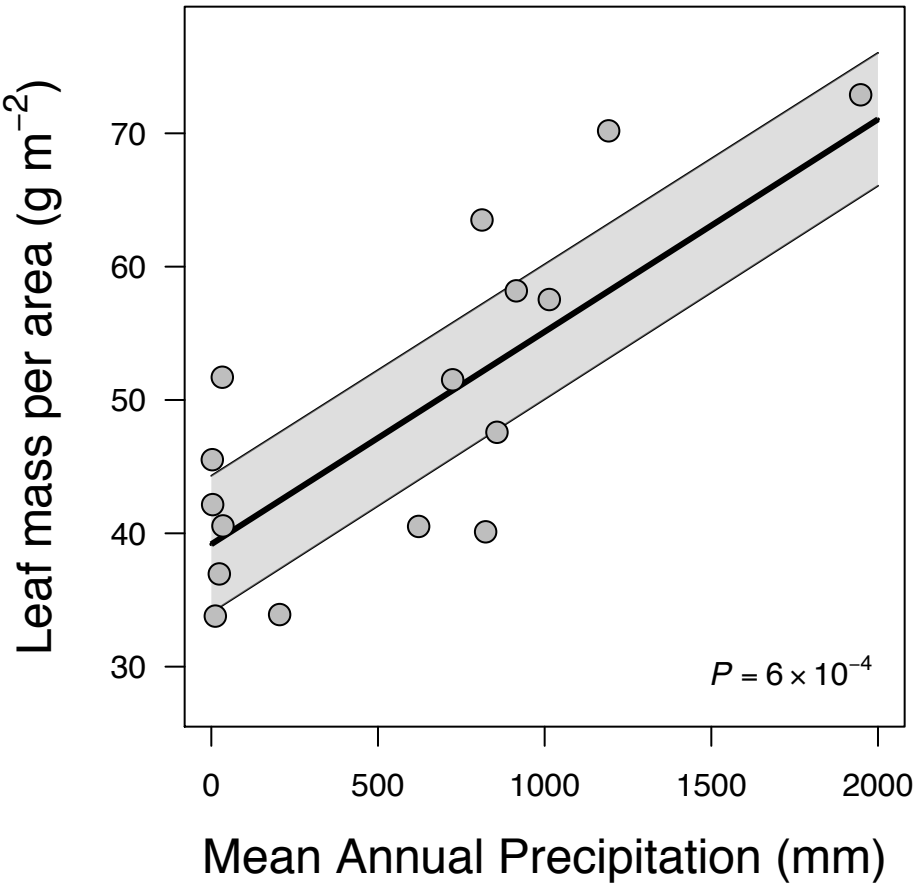

575

576 **Figure S3**: Leaf mass per area (*LMA*) was positively correlated with mean annual precipitation.

577 Each point shows the climate at habitat of origin for a different wild tomato taxon and its *LMA*,

578 averaged from multiple individuals in the experiment. There was a significant positive

579 correlation between PC1 and precipitation. All *P*-values are from phylogenetic linear regression.

580

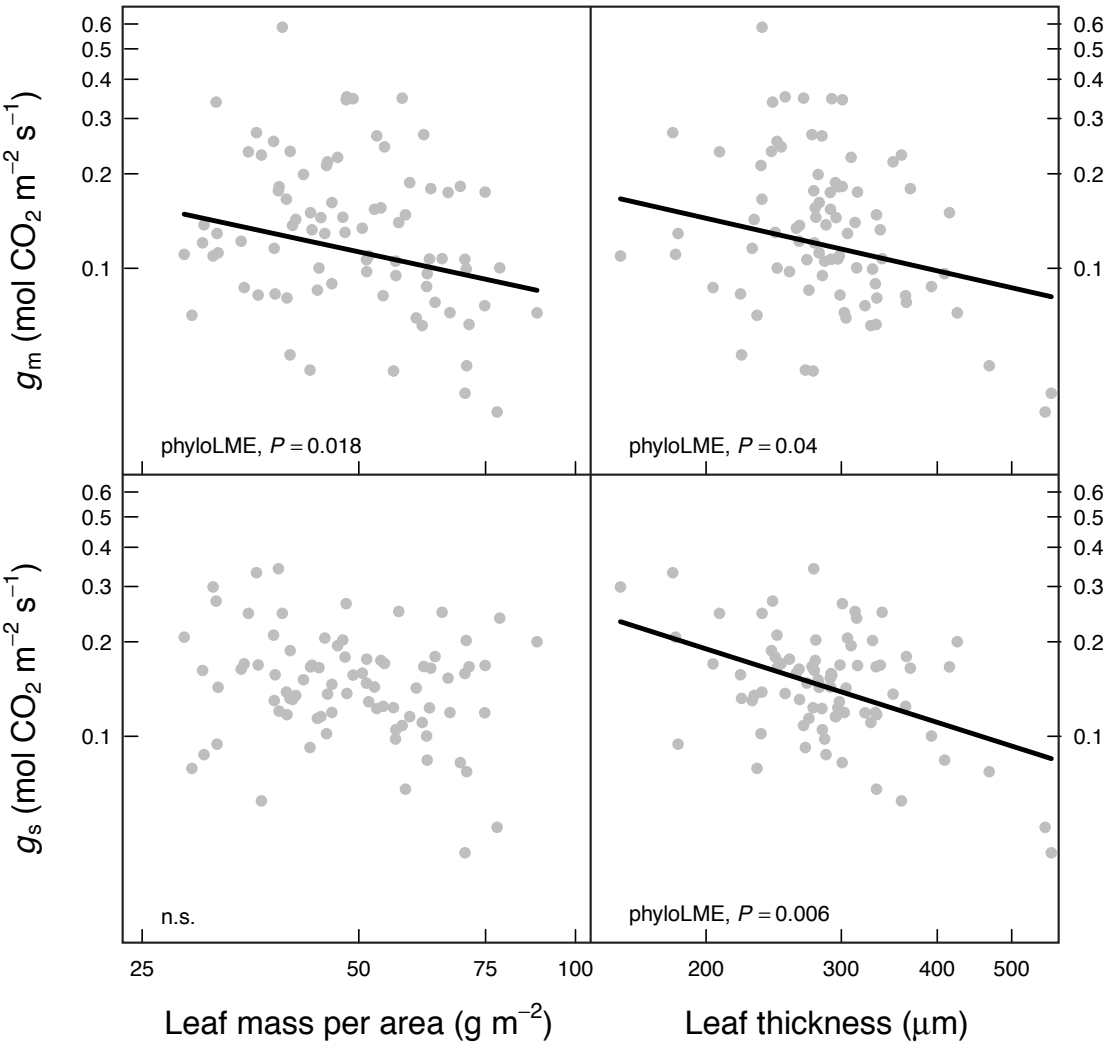

581

582 **Figure S4:** Bulk leaf structure (leaf mass per area [*LMA*] and leaf thickness [*LT*]) weakly

583 constrain leaf CO_2 diffusive conductance through stomata (g_s) and mesophyll (g_s). Each point is

584 data from one of 80 individual plants across 19 wild and cultivated tomato taxa. Panels A. and B.

585 show that diffusion through mesophyll (g_m, mesophyll conductance) was limited by higher *LMA*

586 and *LT*. Additionally, *LT* (panel D.), but not *LMA* (Panel C.) were associated with decreased

587 stomatal conductance (g_s) parameters. Fitted lines are based on Bayesian phylogenetic mixed

588 models treating Species as a random effect. Mixed models with *LT* also included *LDMC*, but this
589 did not have a significant effect (results not shown). All *P*-values are based on 10^4 MCMC
590 samples from the posterior distribution of the model.
591

Methods S1

Gas exchange

We used an open path infrared gas exchange analyzer with a 2-cm^2 leaf chamber fluorometer (LI-6400-40, LI-COR Inc., Lincoln, NE, USA) to simultaneously measure leaf gas exchange and chlorophyll *a* fluorescence. To minimize leaf position and age effects, all measurements were made on young, fully-expanded leaves ($\bar{n} = 4.3$, range = [3, 5]). The ambient CO_2 concentration in the chamber (C_a) was 400 µmol CO_2 mol^{-1} air, leaf temperature was 25° C, photosynthetic photon flux density (PPFD) was 1500 µmol m^{-2} s^{-1} with 90:10 red:blue light, and relative humidity was between 40 – 60%. Once a leaf reached steady-state photosynthesis (A) and stomatal conductance (g_s), usually after ~30 min, we measured the response to changing substomatal CO_2 concentrations (C_i) by adjusting the ambient CO_2 concentration in the leaf chamber (C_a). We used 11 concentrations between 0 and 1750 µmol CO_2 mol^{-1} air. The flow rate was 300 µmol s^{-1}. Diffusional leaks for CO_2 were corrected for using the methods of Rodeghiero *et al.* (2007). We observed no differences between diffusion coefficients calculated for leaves of different species or an empty chamber (data not shown).

From fluorescence measurements and $A - C_i$ curves, we determined the net CO_2 assimilation rate at C_a = 400 µmol CO_2 mol^{-1} air (A_N), stomatal conductance (g_s), mesophyll conductance to CO_2 (g_m), and the maximum rate of carboxylation (V_{cmax}). For all analyses, we used g_s and g_m at ambient C_a (400 +/- 5 µmol CO_2 mol^{-1} air) because these values are most ecologically relevant and allowed us to directly analyze how g_s and g_m limited A_N. Photosynthetic rate and stomatal conductance are estimated directly from gas exchange measurements. We estimated mesophyll conductance using from the equation (Harley *et al*. 1992):

$$g_m = \frac{A}{C_i - \frac{\Gamma^*[J+8(A+R_d)]}{J-4(A+R_d)}} \quad \text{(S1)}$$

We measured the mitochondrial respiration rate (R_{dark}) for each plant at predawn and used the common assumption $R_d = R_{dark} / 2$. As described below, we measured the chloroplastic CO_2 compensation point (Γ^*) *in vitro* from two species, *S. lycopersicoides* and *S. lycopersicum* var. *esculentum* cv. 'Roma', one each from the two LSu amino acid sequences among tomato species (see Results). For *S. lycopersicoides* (Rubisco LSu Type 1, Figure S2), we estimated $\Gamma^* = 40.46$ µmol CO_2 mol^{-1} air; for *S. lycopersicum* (Rubisco LSu Type 2, Figure S2) we estimated $\Gamma^* =$ 35.39 µmol CO_2 mol^{-1} air. These values were applied to the other species with the same Rubisco LSu Type (Figure S2).

The electron transport rate of photosystem II (J_f) was calculated from fluorescence measurements as $J_f = \Phi_{PSII} I \alpha \beta$, where Φ_{PSII} is the quantum yield (moles of CO_2 fixed per mole of quanta absorbed) of photosystem II, I is irradiance, α is the leaf light absorptance, and β is the photosystem partitioning factor. Φ_{PSII} was estimated from the chlorophyll fluorescence data. We estimated the product αβ separately for each species using the relationship $\Phi_{PSII} = \frac{\alpha\beta\Phi_{CO_2}}{4}$ under nonphotorespiratory conditions (Genty, Briantis & Baker, 1989). To vary the quantum yield, we measured photosynthetic light response curves under 2% O_2. In summary, we incorporated data on species-specific respiration (R_d), Rubisco kinetics (Γ^*), and light absorptance/photosystem partitioning (αβ) to improve the accuracy of g_m estimates.

Using the calculated values of g_m, we used the relationship:

$$C_c = C_i - A/g_m \quad \text{(S2)}$$

to determine $A - C_c$ curves to estimate the maximum velocity of carboxylation (V_{cmax} [µmol m^{-2} s^{-1}]), which is proportional to the concentration of activated Rubisco. We estimated V_{cmax}

following Long & Bernacchi (2003) from the linear, Rubisco limited portion of the $A - C_c$ curve, empirically determined to be $C_i < 200$ mol CO_2 mol^{-1} air. We used kinetic values from Table 2 (methods described below) to calculate effective Michaelis-Menten constants for each LSu type.

Sequencing the Rubisco large subunit

Total DNA was extracted from fresh leaf tissue using the DNeasy Plant MiniKit (Qiagen). The *rbc*L gene coding for the Rubisco large subunit (LSu) was amplified using primers specifically designed for *Solanum*, the forward primer SoSpaF (5´-ATGAGTTCTAGGGAGGGAT-3´) and the reverse primer So1462R: (5'-GCAGGAAATAAAGAAGGATAAGG-3'). The BioMix Red reaction mix (Bioline Ltd., London, UK) was used to carry out the polymerase chain reaction (PCR) with the following conditions: an initial cycle of 95 °C, 2 min; 55 °C, 30 s; 72 °C, 4 min, followed by 36 cycles of 93 °C, 30 s; 53 °C, 30 s; 72 °C, 3.5 min. PCR products were visualized on 1% agarose gels, purified using the High Pure PCR Product Purification Kit (Roche, Germany) and sequenced with an ABI 3130 Genetic analyzer using the ABI BigDyeTM Terminator Cycle Sequencing Ready Reaction Kit (Applied Biosystems, Foster City, California). Due to the *rbc*L length, sequences were obtained in a two-fragment fashion, using the primer So1462R and the primer rbcL638R (5'-CGCATAAATGGTTGGGAATTC-3') (Chen 1998). Sequence chromatograms were checked and corrected with the Chromas software and the contigs were assembled using BioEdit v7.1.3 software (Hall 1999). MEGA 5 (Tamura *et al*. 2011) was used to convert DNA to amino acid, and to align both sequence types.

Rubisco catalytic characterization

Based on the two different amino acid sequences detected, a representative species for each type was selected, *S. lycopersicoides* for Rubisco LSu Type 1, and a domesticated accession *S. lycopersicum* var. *esculentum* cv. 'Roma' for the Rubisco LSu Type 2. We characterized Rubisco kinetics following Galmés *et al.* (2014). Rates of Rubisco $^{14}CO_2$ fixation using fresh leaf protein extract were measured in 7 ml septum-capped scintillation vials, containing reaction buffer (yielding final concentrations of 100 mM Bicine-NaOH, pH 8.0, 20 mM $MgCl_2$, 0.4 mM RuBP and ca. 100 W-A units of carbonic anhydrase) and one of nine different concentrations of CO_2 (0-80 μM, each with a specific radioactivity of 3.7 x 10^{10} Bq mol^{-1}), each at two concentrations of O_2 (0 and 21% v/v), as described previously (Parry *et al.* 2007). Assays (1.0 ml total volume) were started by the addition of activated leaf extract, and the maximum velocity of carboxylase activity (V_{max}) together with the Michaelis-Menten constant (K_m) for CO_2 (K_c) determined from the fitted data. The K_m for the oxygenase activity was calculated from the relationship $K_{c,(21\%O2)} = K_{c,(0\%O2)} \cdot (1 + [O_2]/K_o)$. The $[O_2]$ was assumed to be 265 μM, but corrected for partial pressure by taking account of the atmospheric pressure and water saturated vapor pressure. Replicate measurements ($n = 4$) were made using protein preparations from different leaves of different individuals. For each sample, the maximum rate of carboxylation (k^c_{cat}) was extrapolated from the corresponding V_{max} value after allowance was made for the Rubisco active site concentration, as determined by [^{14}C]CPBP binding (Yokota & Canvin 1985). Rubisco CO_2/O_2 specificity ($S_{c/o}$) was measured as described previously (Galmés *et al*. 2005) using enzyme purified by polyethylene glycol (PEG) precipitation and ion exchange chromatography, and the values given for each species were the mean of 7-8 repeated determinations. The maximum oxygenation rate (k^o_{cat}) was calculated using the equation $S_{c/o} = (k^c_{cat} / K_c)/(k^o_{cat} / K_o)$. All kinetic measurements were performed at 25ºC.

679

680 **Results S1: Sequence comparisons reveal two Rubisco LSu types in tomatoes**

681

682 We identified five mutations in the *rbc*L gene sequence (Figure S2), encoding for the Rubisco
683 LSu. However, only one of these five mutations altered the amino acid sequence. The limited
684 variability in LSu among tomato species contrasts with previous studies reporting large
685 variability among closely related taxa in *Limonium* (Galmés *et al*. 2014), *Schidea* (Kapralov &
686 Filatov 2006), *Amanthaceae* (Kapralov *et al*. 2012), and *Quercus* (Hermida-Carrera *et al*. unpub.
687 data). The single mutation leading to a different amino acid sequence for the LSu at position 230
688 (Figure S2) resulted in improved $S_{c/o}$ (i.e., higher specificity of the enzyme for CO_2), but did not
689 reduce the enzyme velocity (k^c_{cat}; Table 2). The same amino acid replacement A230 to T230 was
690 observed in the Hawaiian endemic genus *Schiedea* (Kapralov & Filatov 2006). *Schiedea*
691 represents one of the largest plant adaptive radiations on Hawaii and, similarly to the wild
692 species of tomato in the present study, comprises closely related species with a broad range of
693 morphological and ecological forms, inhabiting diverse environments from rainforest to desert-
694 like conditions. According to Kellogg & Juliano (1997), residue 230 interacts with the βA-βB
695 loop of small subunit, and replacement A230 to T230 causes a decrease in the hydrophobicity of
696 the residue with effects in the stability at this position.

697 We designate the sequence associated with lower $S_{c/o}$ 'Rubisco LSu Type 1' and that with
698 higher $S_{c/o}$ 'Rubisco LSu Type 2'. Interestingly, the Rubisco LSu Type 2 occurs in the closest
699 wild relatives of the domesticated tomato (i.e., from here on "the domesticated clade": *S.*
700 *pimpinellifolium*, *S. cheesmaniae*, *S. galapagense*, *S. lycopersicum* var. *cerasiforme*, and the
701 domesticated accessions; see Figure S2), maybe pointing to this biochemical improvement at

Rubisco level to one of the reasons triggering the diversification of the most recent tomato species, and from which the domesticated tomato was originated. Also, the lack of DNA mutations in the *rbc*L among those species could reflect a very recent occurrence of this Rubisco LSu type.

The phylogenetic relationship among sections *Lycopersicoides*, *Juglandifolia* and *Lycopersicon* is consistent both based on nuclear markers and cpDNA markers (Peralta *et al*. 2008; Robertson *et al*. 2011), and indicates that sect. *Lycopersicoides* diverged before sect. *Juglandifolia* (Figure 1). Therefore, since the cpDNA of sect. *Lycopersicon* is identical to that of sect. *Lycopersicoides* but different to that of sect. *Juglandifolia*, mutations in the latter section may have occurred after the split from sect. *Lycopersicon*, which maintained the original sect. *Lycopersicoides* cpDNA. Therefore, sect. *Juglandifolia* shows two exclusive mutations (in positions 81 and 255), and within *S. juglandifolium* has a third one (in position 573; Figure S2), which shows that this section has the most divergent *rbc*L sequences among tomatoes. However, these mutations did not alter the amino acid sequence of the LSu, suggesting that negative selection on the majority of nonsynonymous substitutions.

As an exception to the above is S. *habrochaites*, which diverged early on in the sect. *Lycopersicon* clade with *S. pennellii*. This species has the Rubisco LSu Type 2, but a different, exclusive haplotype as compared to that in the domesticated clade. Therefore, it appears that the mutation in the DNA position 688, resulting in the amino acid change leading to Rubisco LSu Type 2, may have occurred independently in *S. habrochaites* and in the domesticated clade species. Evidence for convergence is reinforced by the mutation in the DNA position 822, which occurs exclusively in all the domesticated clade species, whereas the *S. habrochaites* haplotype resembles other species in the Rubisco LSu Type 1 at this position. This apparently convergent

725 origin of the mutation leading to an improved Rubisco would reflect 1) the importance of
726 maintaining the ancestral (i.e., Type 1, sect. *Lycopersicoides*) Rubisco LSu across the tomato
727 radiation, because it has been maintained in most species, and 2) little positive selection on the
728 LSu, because only a single amino acid change was detected, in the amino acid position 230, and
729 moreover, it may have occurred twice.
730

731 **References S1**

732 Galmés J., J. Flexas, A.J. Keys, J. Cifre, R.A.C. Mitchell, P.J. Madgwick, R.P. Haslam, H.
733 Medrano, M.A.J. Parry. (2005). Rubisco specificity factor tends to be larger in plant
734 species from drier habitats and in species with persistent leaves. *Plant, Cell &*
735 *Environment,* 28, 571–579.
736 Galmés, J. *et al.* (2014). Environmentally driven evolution of Rubisco and improved
737 photosynthesis and growth within the C_3 genus *Limonium* (Plumbaginaceae). *New Phyto.,*
738 203, 989-999.
739 Genty B., J.M. Briantais, N.R. Baker. (1989). The relationship between the quantum yield of
740 photosynthetic electron transport and quenching of chlorophyll fluorescence. *Biochimica*
741 *et Biophysica Acta* 990, 87–92.
742 Hall, T. A. (1999). BioEdit: a user-friendly biological sequence alignment editor and analysis
743 program for Windows 95/98/NT. *Nucleic Acids Symposium Series*, 41, 95-98.
744 Harley, P.C., F. Loreto, G. Di Marco, T.D. Sharkey. (1992). Theoretical considerations when
745 estimating the mesophyll conductance to CO_2 flux by analysis of the response of
746 photosynthesis to CO_2. *Plant Physiology,* 98, 1429–1436.

747 Kellogg E.A. & N.D. Juliano. (1997). The structure and function of RuBisCO and their
748 implications for systematic studies. *Am J Bot,* 84, 413–428.
749 Kapralov, M.V. & D.A. Filatov. (2006). Molecular adaptations during adaptive radiation in the
750 Hawaiian endemic genus *Schiedea*. PLoS ONE, 1, e8.
751 Kapralov M.V., J.A.C. Smith, D.A. Filatov. (2012). Rubisco evolution in C_4 eudicots: an
752 analysis of Amaranthaceae *sensu lato*. PLoS ONE, 7, e52974.
753 Parry, M.A.J., P.J. Madgwick, J.F.C. Carvalho, P.J. Andralojc. (2007). Prospects for increasing
754 photosynthesis by overcoming the limitations of Rubisco. *Journal of Agricultural Science*
755 145, 31–43.
756 Peralta, I.E. *et al.* (2008). The taxonomy of tomatoes: a revision of wild tomatoes (*Solanum*
757 section *Lycopersicon*) and their outgroup relatives in sections *Juglandifolium* and
758 *Lycopersicoides*. *Syst. Bot. Monogr.,* 84, 1-186.
759 Robertson, K.A., E.E. Goldberg, B. Igić. (2011). Comparative evidence for the correlated
760 evolution of polyploidy and self-compatibility in Solanaceae. *Evolution* 65, 139-155.
761 Tamura K.D., D. Peterson, N. Peterson, G. Strecher, M. Nei, S. Kumar. (2011). MEGA5:
762 Molecular Evolutionary Genetics Analysis using maximum likelihood, evolutionary
763 distance, and maximum parsimony methods. *Molecular Biology and Evolution* 28, 2731–
764 2739.
765 Yokota A. & D.T. Canvin. (1985). Ribulose bisphosphate carboxylase/oxygenase content
766 determined with [^{14}C] carboxypentitol bisphosphate in plants and algae. *Plant*
767 *Physiology,* 77, 735–739.
768
769